

Strange-Nonchaotic-Attractor-Like Behaviors in Coupled Map Systems*

SHI Peng-Liang,¹ HE Dai-Hai,¹ FU Wu-Liu,² KANG Wei¹ and HU Gang¹

¹Department of Physics, Beijing Normal University, Beijing 100875, China

²Department of Physics, Fuzhou Normal College, Fuzhou 344000, Jiangxi Province, China

(Received January 2, 2001)

Abstract In a coupled map system, an attractor which seems to be strange nonchaotic attractor (SNA) is discovered for nonzero measure in parameter range. The attractor has nonpositive Lyapunov exponent (LE) and discrete structure. We call it strange-nonchaotic-attractor-like (SNA-like) behavior because the size of its discrete structure decreases with the computing precision increasing and the true SNA does not change. The SNA-like behavior in the autonomous system is born when the truncation error of round-off is amplified to the size of the discrete part of the attractor during the long time interval of positive local LE. The SNA-like behavior is easily mistaken for a true SNA judging merely from the largest LE and the phase portrait in double precision computing. In non-autonomous system an SNA-like attractor is also found.

PACS numbers: 05.45.+b

Key words: strange nonchaotic attractor, truncation error, logistic map

1 Introduction

Strange nonchaotic attractor (SNA) has attracted much attention in recent two decades.^[1] Up to now, all SNAs are found in non-autonomous systems, not in autonomous ones. Autonomous systems cannot be divided into one driving and one response parts in mathematical language;^[2] but non-autonomous systems can. It is believed that the SNA can appear in quasiperiodically forced differential systems, or periodically driven map systems. Anishchenko *et al.* found that an SNA can exist in autonomous system,^[3,4] but this conclusion was soon denied by Pikovsky and Feudel after computing Lyapunov exponents (LEs) in higher precision.^[2]

In another aspect, the shadowing lemma considers the problem with profound mathematical background in what extent we can rely on the computer-generated orbit.^[5–7] For a hyperbolic system in chaotic case although a numerical trajectory diverges exponentially from the true trajectory with the same initial condition, there exists a true (i.e. errorless) trajectory with a slightly different initial condition that stays near (shadows) the numerical trajectory. The shadowing lemma states that for each nonzero distance ε there exists an error magnitude δ such that each δ pseudotrajectory can be ε shadowed. Furthermore, under the hyperbolicity assumption, each such pseudotrajectory can be continuously shadowed within ε . Nonchaotic systems do not yield long-term exponential divergence of solutions, i.e., a small initial error leads to small or slowly growing errors for all time. However, it is reported recently that extremely weak noise is sufficient to induce dynamical complexity in an SNA.^[6] It is identified that local LEs (sometimes called finite-time LEs)

fluctuating about zero will cause nonexistence of shadowing trajectories,^[7] and then the local LEs have become a focus in recent years.^[6–8]

In Sec. 2 an SNA and a novel SNA-like behavior are discussed in nonautonomous systems. The similar behavior for an autonomous system will be discussed in Sec. 3 in details. In the last section some conclusions are given.

2 SNA and SNA-Like Behavior in Nonautonomous System

There are many models which have true SNAs, and we can give a typical example, a periodically forced circle map,^[9]

$$\begin{aligned}x_{n+1} &= x_n + K + \frac{V}{2\pi} \sin 2\pi x_n + \frac{C}{2\pi} \cos 2\pi \theta_n \bmod 1, \\ \theta_{n+1} &= \theta_n + \omega \bmod 1,\end{aligned}\quad (1)$$

here we fix parameters

$$K = 0.2841, \quad V = 0.95,$$

and study the system behavior at $C = 1.1304$. We plot the phase portraits in Figs 1a and 1b for the 16-digital and 100-digital precisions, respectively. The attractor is nondifferential and the largest LE of the system is nonpositive, the attractor is thus an SNA. It is apparent that figures 1a and 1b are practically the same. The phase portrait is not changed by increasing the computing precision. The attractor in Fig. 1 is then regarded as a true SNA in a nonautonomous system.

Now let us consider a different model which has also quasiperiodically driving, a logistic map driven by a low

*The project supported by National Natural Science Foundation of China, the Nonlinear Science Project of China, and the Foundation of Doctoral Training of Educational Bureau of China

frequency periodical force,

$$\begin{aligned} x_{n+1} &= ax_n(1-x_n) + b \cos(2\pi\theta_n), \\ \theta_{n+1} &= \theta_n + \omega \bmod 1, \end{aligned} \quad (2)$$

where we take $\omega = 0.001 \times (\sqrt{5} - 1)/2$, $b = 0.1$ and $a = 3.4$. Now we also plot the phase portraits of model (2) in Figs 2a and 2b for the 16-digital and 100-digital, precisions respectively. The phase portrait of Fig. 2a looks strange. Together with the nonpositive LEs, figure 2a seems to indicate an SNA. However the phase portrait in Fig. 2b shows a well-behaved torus for higher computation precision. In order to make clear the mechanism yielding the distinctive behaviors of Figs 2a and 2b, we plot the deviations $\delta = |x' - x| + |\theta' - \theta|$ between two adjacent trajectories in Fig. 3 where $|\theta' - \theta|$ keeps constant due to the periodicity of the driving. In Fig. 3a the computation is performed in the double precision. For various small initial deviations the distances increase as time and quickly reach the size of the attractor in certain time intervals, ir- regarding the distances of the initial deviations. However, in Fig. 3b for 100-digital precision, for small initial deviations, δ increases to the order of 10^{-17} . Consequently, the nonsmooth part cannot be observed in the phase portrait of Fig. 2b. The size of the nondifferential part can be

further reduced by increasing the computing precision to even higher. In this sense we understand that the portrait of Fig. 2a is not a true SNA but a round-off error-induced SNA-like pattern, which will be called SNA-like behavior. The features in Figs 2 and 3 can be well explained by the behavior of the so-called local Lyapunov exponents. For system (2) there are two LEs, one zero and the other negative. It seems that there is not any expansion mechanism for the distance of any neighbor trajectories. However, local LE analysis can demonstrate this mechanism. In Figs 3c and 3d the two-step second local LEs (LE-2) are plotted by taking 16-digital and 100-digital precisions, respectively. By LE-2 we mean that the expansion rate in the exponential exponent is computed by averaging two steps only (in comparison, conventional LE is computed, based on the average of infinitely many steps). By comparing Figs 3a and 3b with Figs 3c and 3d, we find that the deviation expanding time intervals in Figs 3a and 3b exactly coincide with the intervals of positive two-step LE in Figs 3c and 3d. The high local instability in the positive local LE region greatly amplifies the truncation error, and dramatically changes the structure of the attractor if the computing precision is not high enough.

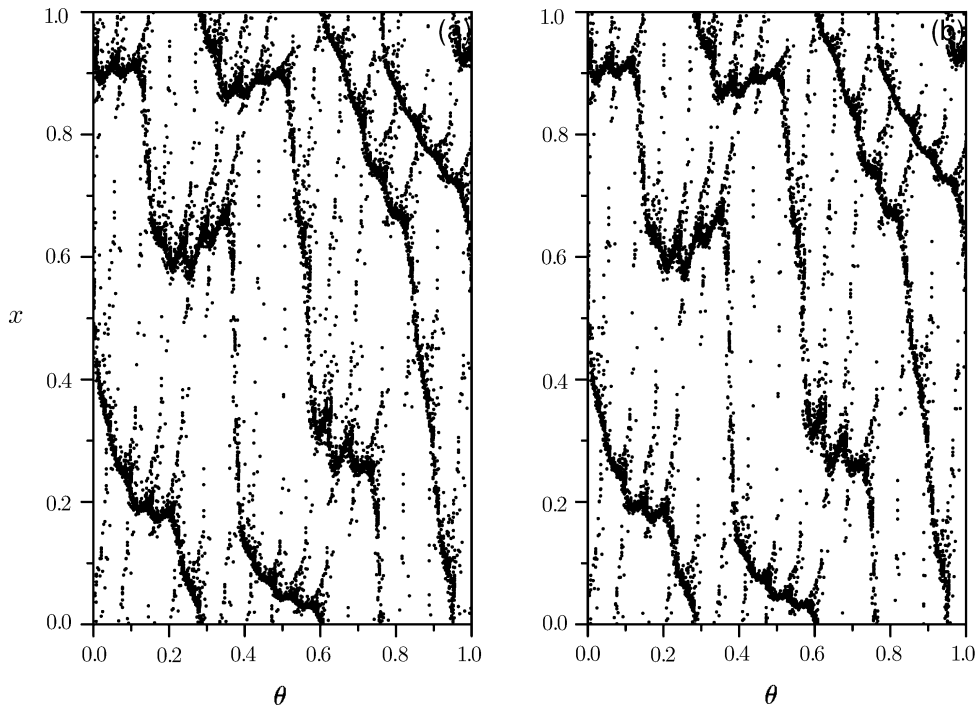


Fig. 1 The phase portraits of SNA of Eqs (1), $K = 0.2841$, $V = 0.95$, $C = 1.1304$. (a) 16-digital computation precision; (b) 100-digital computation precision.

In this section we have shown both SNA and SNA-like behaviors of nonlinear and quasiperiodically driven maps. In the latter case, the system attractor would be a smooth torus if we apply an infinitely high computation precision. However, in actual computations (usually, double precision computations) and in experiments, finite round-off error and noises are inevitable, then one can see only seemingly SNA behavior. This strange behavior is due to positive local LEs of some modes with truly negative LEs.^[10]

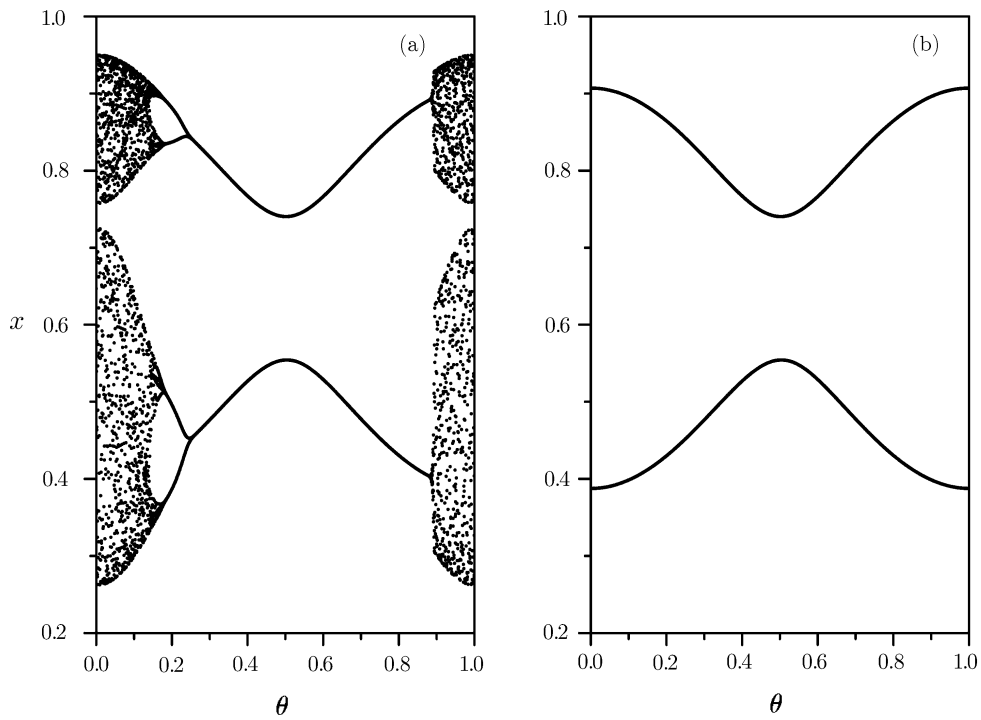


Fig. 2 The same as Figs 1a and 1b, respectively, but with Eqs (2) computed, $a = 3.4$, $b = 0.1$ and $\omega = 0.001 \times (\sqrt{5} - 1)/2$. The same parameters will be used for all figures of Figs 2–6.

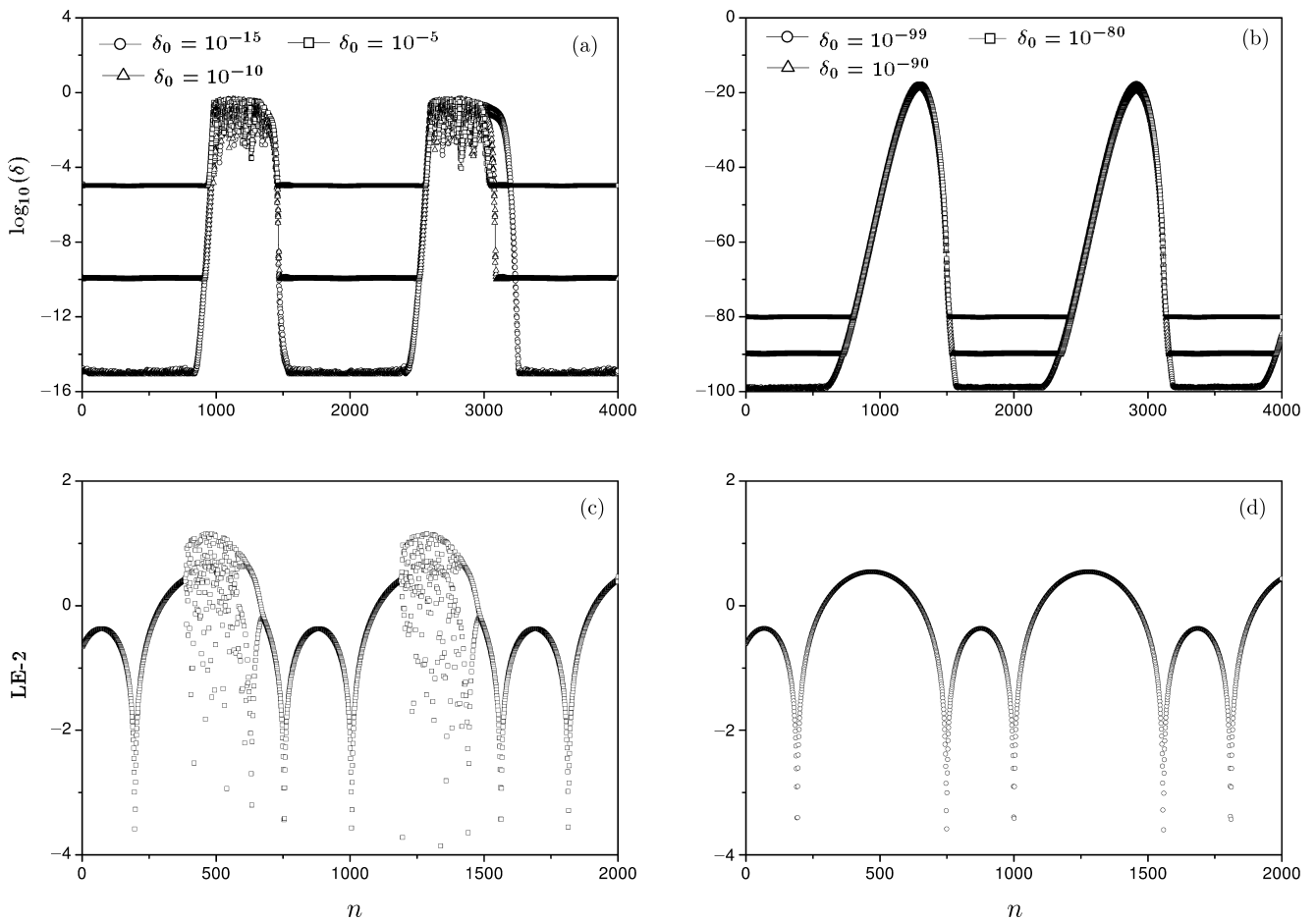


Fig. 3 The minute deviations δ vs. time for different initial deviations in Figs 3a and 3b, (a) 16-digital computation; (b) 100-digital computation. The second two-step local LE vs. n for Eqs (2) in Figs 3c and 3d, (c) 16-digital computation and (d) 100-digital computation precisions.

3 The SNA-Like Behavior in Autonomous System

Now we introduce a coupling from x_n to θ_n , and modify Eqs (2) to an autonomous coupled maps,

$$\begin{aligned} x_{n+1} &= ax_n(1-x_n) + b \cos 2\pi\theta_n, \\ \theta_{n+1} &= \theta_n + \omega + cx_n \text{ mod } 1, \end{aligned} \quad (3)$$

which reduces to Eq. (1) for $c = 0$. In the model we fix a , b , ω as in Eqs (2) and vary c only as our control parameter. It is extensively accepted that SNA can never appear in autonomous systems, including differential equations and maps. It is interesting to see whether SNA-like behavior can be observed in such the systems.

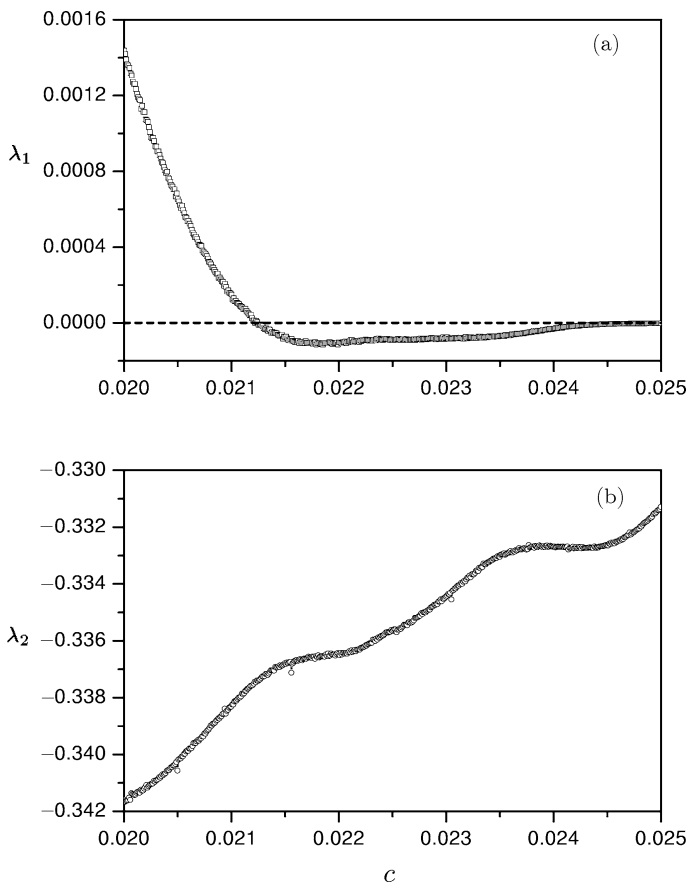


Fig. 4 The LEs $\lambda_{1,2}$ of Eqs (3) plotted vs. c , respectively.

Using the HQR method,^[11] we calculate the LEs λ_1 and $\lambda_2 < \lambda_1$ vs. c in Figs 4a and 4b, respectively, in 16-digital precision (i.e., double precision). There is a parameter window of $\lambda_1 < 0$ ($0.0213 < c < 0.024$). Now we choose, arbitrarily, in the negative λ_1 region $c = 0.022$ for further detecting the system behavior and plot the phase portrait in Fig. 5a in double precision. Strange attractor is apparently observed. It is interesting to further investigate whether the phase portrait in Fig. 5a is a true SNA, or is only an SNA-like attractor. In order to do so we go again to high precision simulation of Maple VI algo-

rithm. We fix our parameters being the same as those in Fig. 5a, and run the system by using 100-digital precision in Fig. 5b. The phase portrait clearly shows a smooth torus. Thus, figure 5a presents an SNA-like attractor exactly the same as Fig. 2a. The difference between Fig. 2 and Fig. 5 is that in the latter case the system is a coupled autonomous map, and then not any true SNA has been found for such the systems. Now we have shown that SNA-like attractors can appear in both nonautonomous and autonomous map systems.

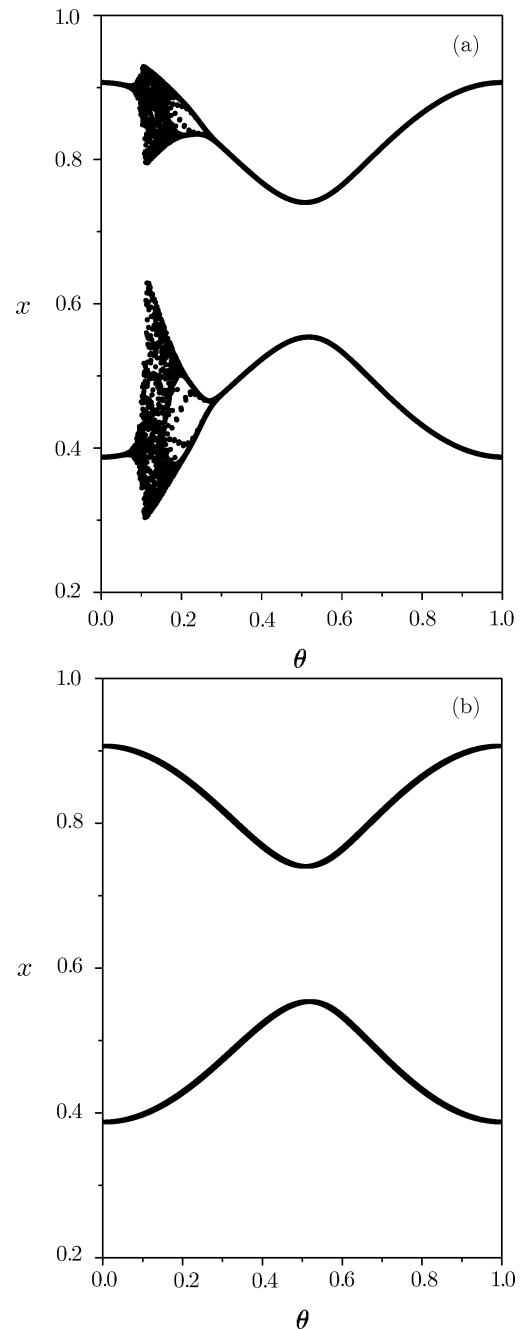


Fig. 5 The same as Figs 2a and 2b, respectively, with Eqs (3) computed, $c = 0.022$.

The mechanism underlying the SNA-like behavior of

autonomous systems (Fig. 5) is the same as that for nonautonomous systems (Fig. 2). In the former case, the micronoise of the round-off has the same chance as the latter to be enlarged enough to lead the strangeness observable in attractor in the double precision computation. In Figs 6a and 6b we do the same computations as in Figs 3a and 3b, respectively, with the nonautonomous map model (2) replaced by the autonomous one (3). With the double precision (16-digital precision) the distances between neighbor trajectories can quickly increase to the order of the attractor size in certain time intervals, no matter how small the initial deviations are. In Fig. 6b for 100-digital precision the distances between any neighbor trajectories can increase only to the order of 10^{-82} so long as the initial deviations δ_0 are smaller than 10^{-82} . In the case of $\delta_0 > 10^{-80}$, the distance between these neighbor trajectories δ_n generically remains at the same order as δ_0 , this coincides with the largest zero LE ($\lambda_1 = 0$). One can reasonably expect that for even higher computation precision, the upper height in Fig. 6b can be reduced, and this height goes to zero if infinite computation precision

and small enough initial deviation can be taken (of course, this precision can never be reached). The above features of Figs 6 are exactly the same as those in Figs 3. Nevertheless, there is an essential difference between Figs 3 and 6. In Figs 3, for each δ_0 the various δ valleys have the same value of $|\Delta\theta|_{n=0}$. The reason is that the deviation of $|\Delta x|$ drops to zero in these flat valleys while $|\Delta\theta_n| = |\Delta\theta_0|$ since this quantity does not change without the coupling from x_n to θ_n . However, in Fig. 6 the case is more interesting, both Δx_n and $\Delta\theta_n$ change all the time, and δ_n varies in the flat valleys of Fig. 6, and finally δ_n saturates to a value with certain fluctuation practically independent of their initial deviations. In Figs 6c and 6d we plot the two-step local LE (LE-2) of λ_2 vs. time for the double precision and 100-digital precision, respectively. We again find that the peak and flat valley parts in Figs 6a and 6b well coincide with the positive and negative local LE of λ_2 . Obviously, the deviation expansion in certain time intervals is due to the positive local LE in the given intervals.

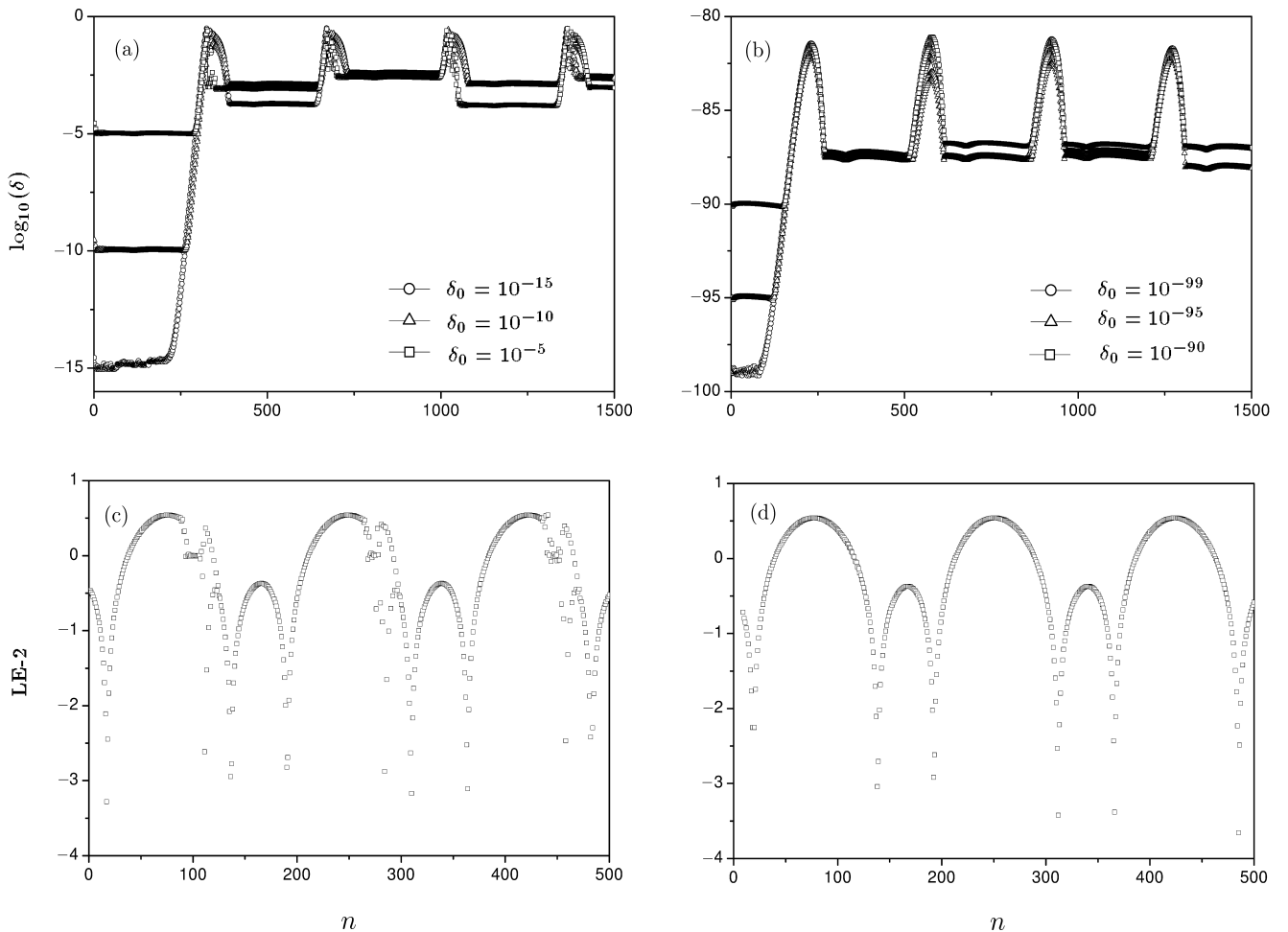


Fig. 6 The same as Figs 3a–3d, but with Eqs (3) computed.

4 Conclusions

In our models an SNA-like behavior is found in both nonautonomous and autonomous systems in double precision computing. In 100-digital precision the system attractors become smooth curves. It is the truncated error of round-off during the computing process that turns a torus into an attractor with the strange behavior. The reason for this SNA-like feature of our systems is that the second negative LE has positive local LE in a long time interval and causes an enormous amplification of small round-off error or noise. This local instability magnifies the mi-

croise into the observable strangeness of the attractors. Based on the shadow lemma, this map is not robustly hyperbolic so that the pseudo-orbit generated by computers in double precision cannot be shadowed by the true orbit.^[12] We would like to emphasize that the SNA-like feature can be easily found in both computer simulations and realistic experiments since finite computer truncation errors and noises definitely exist. Therefore, a thorough investigation in this direction, especially, in the role played by the positive local LE of some negative LEs, is of great significance.

References

- [1] C. Grebogi, E. Ott, S. Pelikan and J.A. Yorke, *Physica* **D13** (1984) 261; C. Grebogi, E. Ott, F.J. Romeiras and J.A. Yorke, *Phys. Rev.* **A36** (1987) 5365; F.J. Romeiras, A. Bondeson, E. Ott, T.M. Anstonsen and C. Grebogi, *Physica* **D26** (1987) 277; F.J. Romeiras and E. Ott, *Phys. Rev.* **A35** (1987) 4404; J.F. Heagy and S.M. Hammel, *Physica* **D70** (1994) 140; L. Ying-Cheng, *Phys. Rev.* **E53** (1996) 57; A. Prasad, V. Mehra and R. Ramaswamy, *Phys. Rev.* **E57** (1998) 1576; T. Nishikawa and K. Kaneko, *Phys. Rev.* **E54** (1996) 6114; Zhi-Gang ZHENG, Bam-Bi HU and Gang HU, *Commun. Theor. Phys. (Beijing, China)* **33** (2000) 191.
- [2] A. Pikosky and U. Feudel, *Phys. Rev.* **E56** (1997) 7320.
- [3] V.S. Anishchenko, T.E. Vadivasova and O. Sosnovtseva, *Phys. Rev.* **E54** (1996) 3231.
- [4] V.S. Anishchenko, T.E. Vadivasova and O. Sosnovtseva, *Phys. Rev.* **E56** (1997) 7322.
- [5] D.V. Anosov, *Proc. Steklov Inst. Math.* **90** (1967) 1; R. Bowen, *J. Differential Equations* **18** (1975) 333; S.M. Hammel, J.A. York and C. Grebogi, *Bull. Am. Math. Soc.* **19** (1998) 465; C. Grebogi, S.M. Hammel, J.A. York and T. Sauer, *Phys. Rev. Lett.* **65** (1990) 1527; J.M. Sanz-Serna and S. Larsson, *Appl. Num. Math.* **13** (1993) 181.
- [6] I.A. Khovanov, N.A. Khovanova, P.V.E. McClintock, V.S. Anishchenko, *Phys. Lett.* **A268** (2000) 315.
- [7] S. Dawson, C. Grebogi, T. Sauer and J.A. York, *Phys. Rev. Lett.* **73** (1994) 1927; T. Sauer, C. Grebogi and J.A. York, *Phys. Rev. Lett.* **79** (1997) 59.
- [8] B. Eckhardt and Demin Yao, *Physica* **D65** (1993) 100; C. Dellago and Wm. G. Hoover, *Phys. Lett.* **A268** (2000) 330; H. Shibata, *Physica* **A284** (2000) 124.
- [9] A. Pikovsky and U. Feudel, *Chaos* **5** (1995) 253.
- [10] J.W. Shuai and K.W. Wong, *Phys. Rev.* **E57** (1998) 5332; J.W. Shuai and K.W. Wong, *Phys. Rev.* **E59** (1999) 5338; J.W. Shuai, Y. Kashimori, T. Kambara and M. Naito, *Phys. Lett.* **A267** (2000) 335.
- [11] Hubertus F. von Bremen, Firdaus E. Udawadia, Wlodek Proskurowski, *Physica* **D101** (1997) 1; K. Ramasubramanian and M.S. Sriram, *Physica* **D139** (2000) 72; Alan Wolf, Jack B. Swift, Harry L. Swinney and John A. Vastano, *Physica* **D16** (1985) 285.
- [12] V.S. Anishchenko, A.S. Kopeikin, J. Kurths, T.E. Vadivasova and G.I. Strelkova, *Phys. Lett.* **A270** (2000) 301.